Toxicology and Applied Pharmacology 266 (2013) 307–316

Contents lists available at SciVerse ScienceDirect

Toxicology and Applied Pharmacology

journal homepage: www.elsevier.com/locate/ytaap

Phenylbutyric acid protects against carbon tetrachloride-induced hepatic fibrogenesis in mice

Jian-Qing Wang [b,d,1], Xi Chen [c,1], Cheng Zhang [a,1], Li Tao [c], Zhi-Hui Zhang [a], Xiao-Qian Liu [a], Yuan-Bao Xu [a,c], Hua Wang [a], Jun Li [b,*], De-Xiang Xu [a,**]

[a] Department of Toxicology, Anhui Medical University, Hefei, 230032, China
[b] School of Pharmacy, Anhui Medical University, Hefei, 230032, China
[c] First Affiliated Hospital, Anhui Medical University, Hefei 230022, China
[d] Second Affiliated Hospital, Anhui Medical University, Hefei 230601, China

ARTICLE INFO

Article history:
Received 15 June 2012
Revised 17 October 2012
Accepted 5 November 2012
Available online 19 November 2012

Keywords:
Endoplasmic reticulum stress
Unfolded protein response
Carbon tetrachloride
Hepatic fibrosis
Phenylbutyric acid

ABSTRACT

A recent report showed that the unfolded protein response (UPR) signaling was activated in the pathogenesis of carbon tetrachloride (CCl_4)-induced hepatic fibrosis. Phenylbutyric acid (PBA) is a well-known chemical chaperone that inhibits endoplasmic reticulum (ER) stress and unfolded protein response (UPR) signaling. In the present study, we investigated the effects of PBA on CCl_4-induced hepatic fibrosis in mice. All mice were intraperitoneally (i.p.) injected with CCl_4 (0.15 ml/kg BW, twice per week) for 8 weeks. In CCl_4 + PBA group, mice were i.p. injected with PBA (150 mg/kg, twice per day) from the beginning of CCl_4 injection to the end. As expected, PBA significantly attenuated CCl_4-induced hepatic ER stress and UPR activation. Although PBA alleviated, only to a less extent, hepatic necrosis, it obviously inhibited CCl_4-induced tumor necrosis factor alpha (TNF-α) and transforming growth factor beta (TGF-β). Moreover, PBA inhibited CCl_4-induced hepatic nuclear factor kappa B (NF-κB) p65 translocation and extracellular signal-regulated kinase (ERK) and c-Jun N-terminal Kinase (JNK) phosphorylation. Interestingly, CCl_4-induced α-smooth muscle actin (α-SMA), a marker for the initiation phase of HSC activation, was significantly attenuated in mice pretreated with PBA. Correspondingly, CCl_4-induced hepatic collagen (Col)1α1 and Col1α2, markers for the perpetuation phase of HSC activation, were inhibited in PBA-treated mice. Importantly, CCl_4-induced hepatic fibrosis, as determined using Sirius red staining, was obviously attenuated by PBA. In conclusion, PBA prevents CCl_4-induced hepatic fibrosis through inhibiting hepatic inflammatory response and HSC activation.

© 2012 Elsevier Inc. All rights reserved.

Introduction

Hepatic fibrosis results from chronic damage to the liver in conjunction with the accumulation of extracellular matrix (ECM) proteins, which is a characteristic of most types of chronic liver diseases (Bataller and Brenner, 2005). The main causes of hepatic fibrosis include chronic HCV infection, alcohol abuse, cholestasis, and nonalcoholic fatty liver disease (Fracanzani et al., 2011; Mallat et al., 2008; Mencin et al., 2007; Moustafa et al., 2012). Hepatic fibrosis is the result of the wound-healing response of the liver to repeated injury. After an acute liver injury, hepatocytes regenerate and replace the necrotic or apoptotic cells. This process is associated with an inflammatory response. If liver injury persists, hepatic stellate cells (HSCs) undergo a phenotypic transformation to become myofibroblast-like with expression of α-smooth muscle actin (α-SMA) and secretion of ECM composed of various proteoglycans and proteins such as collagen type I. Thus, HSCs are the main ECM-producing cells in the injured liver and play a pivotal role in hepatic fibrogenesis (Friedman, 2010).

Endoplasmic reticulum (ER) is an important organelle required for cell survival and normal cellular function. In the ER, nascent proteins are folded with the assistance of ER chaperones. If nascent proteins in the ER are excessive compared with the reserve of ER chaperones, ER stress occurs. Accumulation of unfolded and misfolded proteins aggregated in the ER lumen causes the activation of a signal response termed the unfolded protein response (UPR) (Wu and Kaufman, 2006). The UPR signaling pathway is mediated by three transmembrane ER proteins: inositol requiring ER-to-nucleus signal kinase (IRE)1, activating transcription factor (ATF)6 and double-stranded

Abbreviations: PBA, phenylbutyric acid; ER, endoplasmic reticulum; UPR, unfolded protein response; α-SMA, α-smooth muscle actin; GRP78, glucose regulated protein 78; IRE1, inositol requiring ER-to-nucleus signal kinase1; eIF2α, alpha subunit of translation initiation factor 2; ATF, activating transcription factor; PERK, double-stranded RNA-activated kinase (PKR)-like ER kinase; Col1a, collagen I alpha; TNF-α, tumor necrosis factor alpha; TGF-β, transforming growth factor beta; NF-κB, nuclear factor-kappa B; MAPK, mitogen-activated protein kinase; JNK, c-Jun N-terminal kinase; ERK, extracellular signal-regulated kinase; Mmp, matrix metalloproteinase; Timp, tissue inhibitor of metalloproteinase.

* Corresponding author.
** Corresponding author. Fax: +86 551 3869179.
E-mail addresses: lijun@ahmu.edu.cn (J. Li), xudex@126.com (D.-X. Xu).
[1] These authors contributed equally to this work.

0041-008X/$ – see front matter © 2012 Elsevier Inc. All rights reserved.
http://dx.doi.org/10.1016/j.taap.2012.11.007

RNA-activated kinase (PKR)-like ER kinase (PERK) (Kohno, 2007). Increasing evidence demonstrates that ER stress plays an important role in the pathogenesis of liver disease (Dara et al., 2011). Indeed, bile acids caused hepatic ER stress and the UPR signaling activation in a model of cholestasis-induced hepatic fibrosis (Tamaki et al., 2008). According to a recent study, ER stress is involved in carbon tetrachloride (CCl_4)-induced hepatic steatosis (Lee et al., 2011). Another recent study showed that the UPR signaling was activated in the pathogenesis of carbon tetrachloride (CCl_4)-induced hepatic fibrosis (Ji et al., 2011).

Phenylbutyric acid (PBA) is a low molecular weight fatty acid that has been used for treatment of urea cycle disorders in children and sickle cell disease (Burlina et al., 2001; Odievre et al., 2007). Numerous studies have demonstrated that PBA acts as a chemical chaperone that inhibits ER stress and the UPR signaling activation (Basseri et al., 2009; Hanada et al., 2007). Indeed, PBA could attenuate ER stress and restore glucose homeostasis in a mouse model of type 2 diabetes (Ozcan et al., 2006). Moreover, PBA inhibits the UPR signaling activation and protects against leptin resistance in the hypothalamus of obese mice (Ozcan et al., 2009). In humans, PBA partially alleviated lipid-induced insulin resistance and β-cell dysfunction (Xiao et al., 2011). According to a recent report, pretreatment with PBA significantly reduced ischemia–reperfusion-induced inflammation, apoptosis and necrosis, and improved liver regeneration through inhibiting the UPR signaling activation (Ben Mosbah et al., 2010). Nevertheless, whether PBA protects against hepatic fibrosis remains to be determined.

The aim of the present study was to investigate the effects of CCl_4-induced hepatic fibrosis in mice. We demonstrate for the first time that PBA inhibits hepatic inflammatory response and HSC activation in the pathogenesis of CCl_4-induced hepatic fibrosis. Moreover, pretreatment with PBA effectively protects against CCl_4-induced hepatic fibrosis.

Materials and methods

Chemicals. Carbon tetrachloride (CCl_4), 4-phenylbutyric acid (PBA), fast green FCF and direct red 80 were purchased from Sigma Chemical Co. (St. Louis, MO). Anti-GRP78, anti-peIF2α antibodies were obtained from Cell Signaling (Beverly, MA), anti-α-SMA monoclonal antibodies were from Sigma Chemical Co. (St. Louis, MO), anti-pIRE1αantibodies were from Thermo Fisher Scientific Inc (Rockford, IL), anti-NF-κB p65, anti-p-JNK, anti-pERK, anti-p-p38, anti-Lamin A/C, anti-α-tubulin antibodies, horseradish peroxidase-conjugated goat anti-rabbit, goat anti-mouse and donkey anti-goat IgGs were from Santa Cruz Biotechnology, Inc (Santa Cruz, CA). TRI reagent was purchased from Molecular Research Center, Inc (Cincinnati, OH), RNase-free DNase, AMV and GoTaq® qPCR master mix were from Promega Corporation (Madison, WI). All specific primers were synthesized by Life Technologies Corporation (Carlsbad, CA). Chemiluminescence (ECL) detection kit was obtained from Thermo Fisher Scientific Inc (Rockford, IL) and polyvinylidene fluoride (PVDF) membrane was from Milipore Corporation (Belford, MA). All other reagents were purchased from Sigma Chemical Co. (St. Louis, MO) if not otherwise stated.

Animals and treatments. Male CD-1 mice (6–8 weeks old, 22–24 g) were purchased from Beijing Vital River (Beijing, China). The animals were allowed free access to food and water at all times and were maintained on a 12-h light/dark cycle in a controlled temperature (20–25 °C) and humidity (50 ± 5%) environment for a period of 1 week before use. Mice were divided into four groups. In CCl_4 alone and CCl_4 + PBA groups, mice were intraperitoneally injected with CCl_4 (0.15 ml/kg BW, twice per week) for 8 weeks. In CCl_4 + PBA group, mice were intraperitoneally injected with PBA (150 mg/kg, dissolved in PBS, twice per day) from the beginning of CCl_4 injection to the end. In control group, mice were intraperitoneally injected with PBS. In PBA alone group, mice were intraperitoneally injected with PBA (150 mg/kg, dissolved in PBS, twice per day) for 8 weeks. All procedures on animals followed the guidelines for humane treatment set by the Association of Laboratory Animal Sciences and the Center for Laboratory Animal Sciences at Anhui Medical University.

Biochemical parameters. The levels of total bilirubin (TBIL), direct bilirubin (DBIL), total bile acid (TBA) and alanine aminotransferase (ALT) in serum were measured using commercially available assay kits according to the manufacturer's instructions.

Histology. Liver tissues were fixed in 4% formalin and embedded in paraffin according to the standard procedure. Paraffin embedded tissues were cut 5 μm thick and stained with hematoxylin and eosin (H & E) for morphological analysis. The degree of necrosis was expressed as the mean of twelve different fields within each slide classified on a scale of 0–3 (normal −0, mild-1, moderate-2, severe-3). The number of inflammatory cells was counted in twelve randomly selected fields from each slide at a magnification of ×400.

Determination of liver fibrosis. Liver fibrosis was quantified with Sirius red staining. Ten-micrometer sections were mounted on glass slides. Sections were deparaffinized and the slides rehydrated. The sections were incubated for 2 h in room temperature with an aqueous solution of saturated picric acid containing 0.1% Fast green FCF and 0.1% direct red 80. Morphology of collagen fibers was captured with a light microscope equipped with a CCD digital camera (DP-71, Olympus). Morphometric analysis for fibrosis quantification was performed using five random low-power images per animal at 100× magnification. The percentages of collagen deposition areas were quantified using NIH ImageJ software (http://rsb.info.nih.gov/ij/).

Isolation of total RNA and real-time RT-PCR. Total RNA was extracted using TRI reagent. RNase-free DNase-treated total RNA (1.0 μg) was reverse-transcribed with AMV. Real-time RT-PCR was performed with a GoTaq® qPCR master mix using gene-specific primers as listed in Table 1. The amplification reactions were carried out on a LightCycler® 480 Instrument (Roche Diagnostics GmbH, Mannheim, Germany) with an initial hold step (95 °C for 5 min) and 50 cycles of a three-step PCR (95 °C for 15 sec, 60 °C for 15 sec, 72 °C for 30 sec). The comparative C_T–method was used to determine the amount of target, normalized to an endogenous reference (gapdh) and relative to a calibrator ($2^{-\Delta\Delta Ct}$) using the Lightcycler 480 software (Roche, version 1.5.0). All RT-PCR experiments were performed in triplicate.

Immunoblots. Either nuclear extracts or hepatic lysates were separated electrophoretically by SDS-PAGE and transferred to a polyvinylidene fluoride membrane. For nuclear extracts, the membranes were incubated for 2 h with NF-κB p65 antibody. For hepatic lysates, the membranes were incubated for 2 h with the following antibodies: α-SMA, GRP78, peIF2α, pIRE1α, p-JNK, pERK and pp38. Lamin A/C and α-tubulin was

Table 1
Oligonucleotide sequence of primers for RT-PCR.

Genes	Forward (5′–3′)	Reverse (5′–3′)
Gapdh	ACCCCAGCAAGGACACTGAGCAAG	GGCCCCTCCTGTTATTATGGGGGT
TGF-β1	CGGGAAGCAGTGCCCGAACC	GGGGGTCAGCAGCCGGTTAC
TNF α	CCCTCCTGGCCAACGGCATG	TCGGGGCAGCCTTGTCCCTT
Col 1α1	CAATGGCACGGCTGTGTGCG	AGCACTCGCCCTCCCGTCTT
Col 1α2	CTCATACAGCCGCGCCCAGG	AGCAGGCGCATGAAGGCGAG
Mmp2	ATGGCTACCGCTGGTGTGGC	CACCTTGCCATCGTTGCGGC
Mmp9	CGGCACGCCTTGGTGTAGCA	AGGCAGAGTAGGAGCGGCCC
Timp1	ATTTCCCCGCCAACTCCGCC	AGGGGGCCATCATGGTATCTGCT
Timp2	CGGGGTCTCGCTGGACGTTG	GCGTGTCCCAGGGCACAATGAA

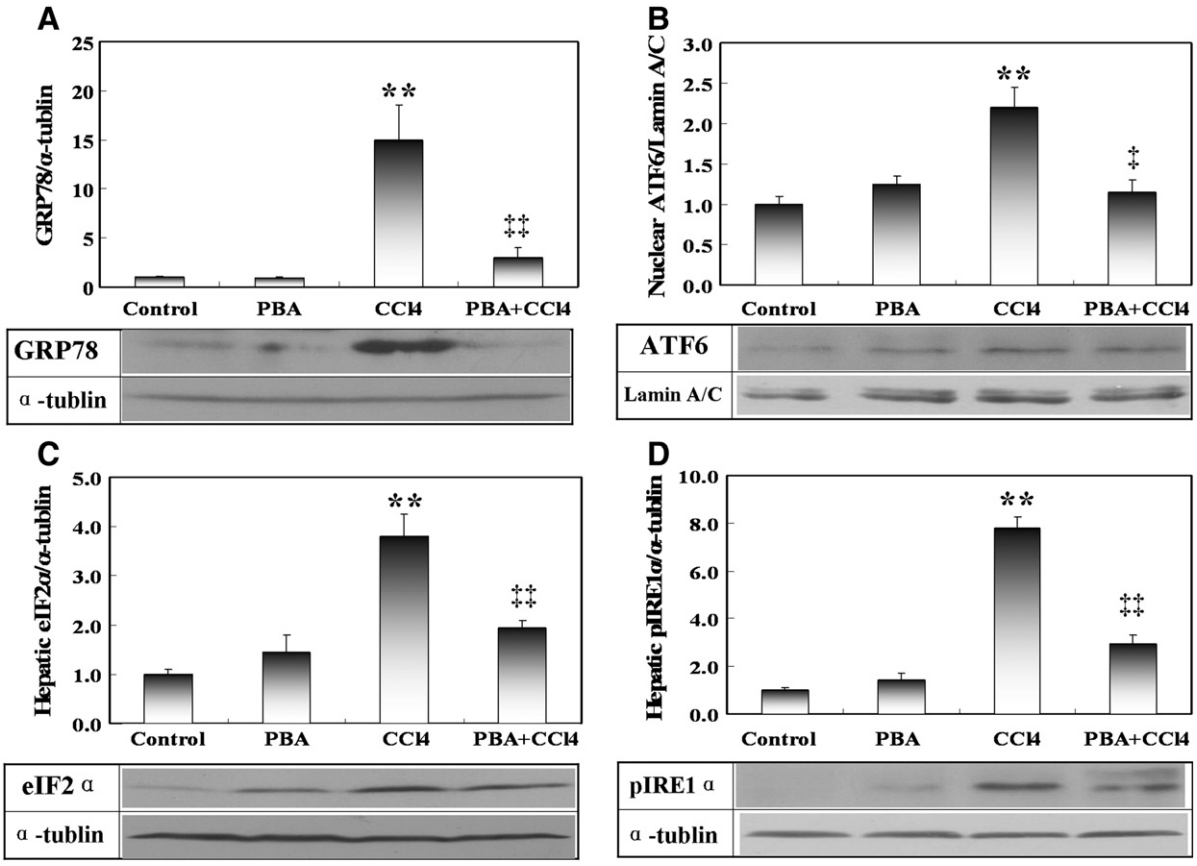

Fig. 1. PBA alleviates CCl_4-induced hepatic ER stress and UPR signaling activation. Mice were intraperitoneally injected with CCl_4 (0.15 ml/kg BW, twice per week) in combination with PBA (150 mg/kg, twice per day) for 8 weeks. Hepatic (A) GRP78, (B) nuclear ATF6, (C) peIF2α and (D) pIRE1α were detected by immunoblotting. All experiments were repeated for four times. Quantitative analyses of scanning densitometry on four different samples were performed. All proteins were normalized to α-tubulin or lamin A/C level in the same samples. All data were expressed as means ± SE. $^{**}P<0.01$ as compared with the control. ‡ $P<0.05$, ‡‡ $P<0.01$ as compared with CCl_4 group.

used as a loading control. After washes in DPBS containing 0.05% Tween-20 four times for 10 min each, the membranes were incubated with goat anti-rabbit IgG antibody for 2 h. The membranes were washed for four times in DPBS containing 0.05% Tween-20 for 10 min each, followed by signal development using an ECL detection kit.

Immunohistochemistry. Paraffin-embedded sections were deparaffinized and rehydrated in a graded ethanol series. After antigen retrieval and quenching of endogenous peroxidase, sections were incubated with anti-α-SMA monoclonal antibodies (1:200 dilution) at 4 °C overnight. The color reaction was developed with HRP-linked polymer detection system and counterstaining with hematoxylin. α-SMA positive cells were counted in twelve randomly selected fields from each slide at a magnification of ×400. Three cross sections were chosen from each liver. The percentage of α-SMA-positive cells was analyzed in six mice from each group.

Hepatic hydroxyproline determination. Hepatic hydroxyproline content was measured as previously described (Reddy and Enwemeka, 1996). Hepatic hydroxyproline content was expressed as μg/g liver.

Statistical analysis. All data were expressed as means ± SE at each point. ANOVA and the Student–Newmann–Keuls post hoc test were used to determine differences among different groups. Differences were considered to be significant only for $P<0.05$.

Results

PBA alleviates CCl_4-induced hepatic ER stress and UPR signaling activation

As shown in Fig. 1A, the expression of hepatic GRP78, an ER chaperone, was significantly upregulated in CCl_4-treated mice. In addition, the level of nuclear ATF6 protein was significantly increased in mice injected with CCl_4 (Fig. 1B). Interestingly, PBA significantly attenuated CCl4-induced elevation of hepatic GRP78 and nuclear ATF6 protein

Table 2
Physiologic and serum parameters.

Parameters	Control ($n=9$)	PBA ($n=9$)	CCl_4 ($n=9$)	PBA + CCl_4 ($n=8$)
Liver weight (g)	2.08 ± 0.09	1.96 ± 0.08	2.54 ± 0.12**	2.11 ± 0.08††
Liver to body weight ratio (%)	4.29 ± 0.13	4.36 ± 0.11	5.94 ± 0.25**	5.06 ± 0.04††
ALT(U/L)	40.78 ± 5.18	37.56 ± 4.12	438.33 ± 73.60**	382.88 ± 83.46
TBIL (μmol/l)	6.79 ± 0.84	7.99 ± 0.54	12.27 ± 1.68**	9.61 ± 0.79
DBIL (μmol/l)	1.41 ± 0.17	1.34 ± 0.18	3.37 ± 0.41**	2.26 ± 0.21†
TBA (μmol/l)	1.40 ± 0.24	1.86 ± 0.26	11.54 ± 1.29**	7.80 ± 1.05†

$^{*}P<0.05$, $^{**}P<0.01$ versus control group; $^{†}P<0.05$, $^{††}P<0.01$ versus CCl_4 group.

(Figs. 1A and B). The effects of PBA on CCl_4-induced hepatic eIF2α and IRE1α phosphorylation are presented in Figs. 1C and D. As expected, the level of hepatic phosphorylated eIF2α was significantly increased in CCl_4-treated mice. In addition, the level of phosphorylated IRE1α was significantly elevated in the liver of mice injected with CCl_4. PBA obviously inhibited CCl_4-induced hepatic eIF2α and IRE1α phosphorylation (Figs. 1C and D).

PBA alleviates CCl_4-induced hepatic necrosis and inflammation

As shown in Table 2, liver weight was significantly increased in mice administered with CCl_4. Interestingly, PBA significantly alleviated CCl_4-induced elevation of liver weight. The effects of PBA on serum biological parameters were then analyzed. As expected, long-term CCl_4 administration significantly increased the levels of serum ALT. Unexpectedly, PBA had little effect on CCl_4-induced elevation of serum ALT levels (Table 2). Further analysis showed that the levels of serum TBIL, DBIL and TBA were significantly increased in mice administered with CCl_4. As shown in Table 2, PBA significantly alleviated CCl_4-induced elevation of serum DBIL and TBA levels. The effects of PBA on CCl_4-induced hepatic histopathological damage are presented in Fig. 2. As expected, numerous inflammatory cells around the necrotic tissue were observed in liver sections from CCl_4-treated mice (Fig. 2B). PBA significantly alleviated CCl_4-induced hepatic inflammation (Fig. 2D). Further analysis showed that the number of inflammatory cells was significantly decreased in liver of mice administered with PBA plus CCl_4 as compared with CCl_4 alone (Fig. 2E). Interestingly, PBA alleviated, only to a less extent, CCl_4-induced hepatic necrosis

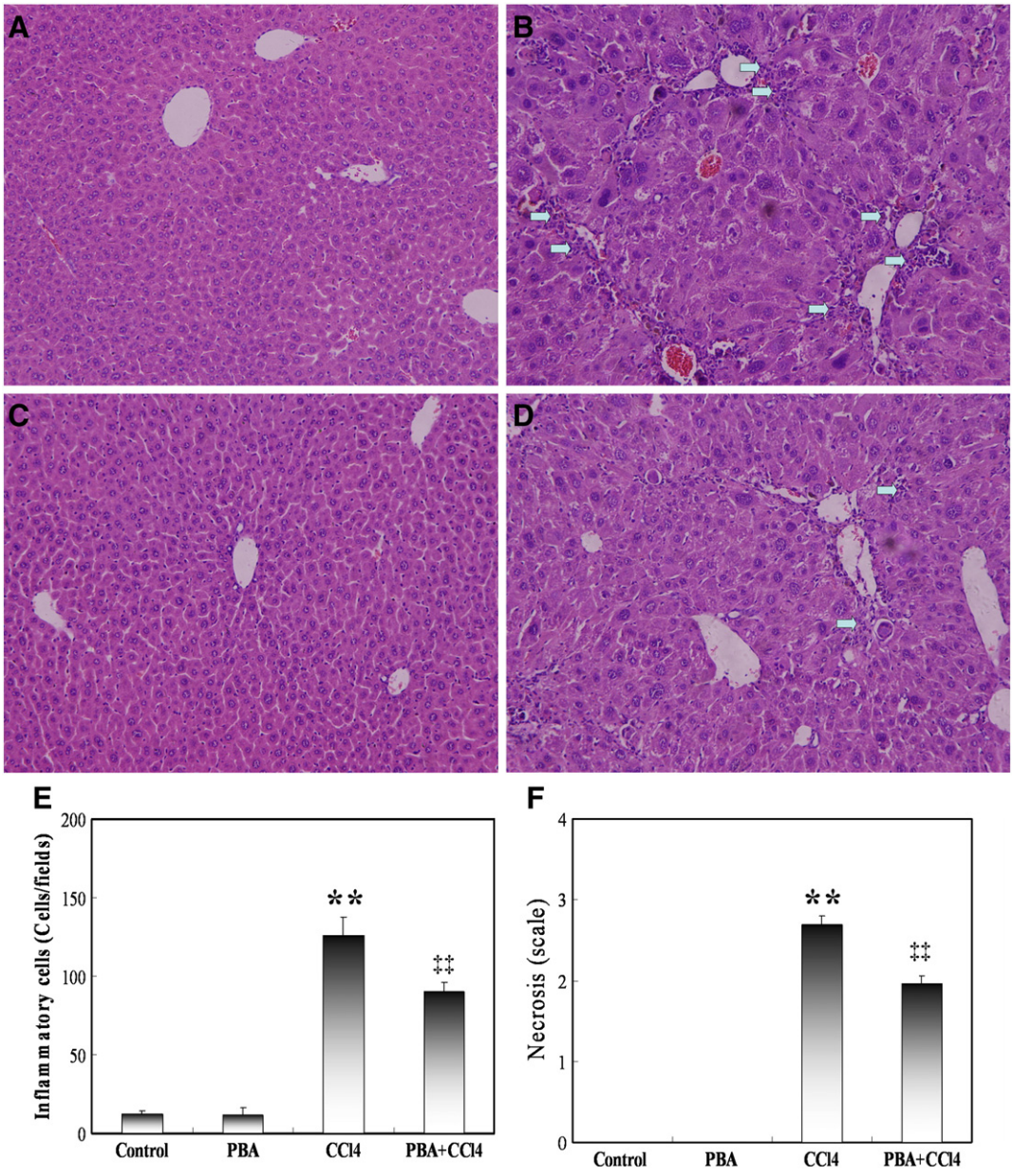

Fig. 2. Effects of PBA on liver histology following long-term CCl_4 treatment. Mice were intraperitoneally injected with CCl_4 (0.15 ml/kg BW, twice per week) in combination with PBA (150 mg/kg, twice per day) for 8 weeks. Representative photomicrographs of liver histology from mice treated with saline (A as control), CCl_4 alone (B), PBA alone (C) and combination of CCl_4 and PBA (D) are shown (H & E, magnification: ×100). Scale bar, 100 μm. Arrows indicate inflammatory cells. The number of inflammatory cells (E) was counted in twelve randomly selected fields from each slide at a magnification of ×400. The degree of necrosis (F) was expressed as the mean of twelve different fields within each slide classified on a scale of 0–3 (normal −0, mild-1, moderate-2, severe-3).

(Fig. 2D). Correspondingly, the grades of necrosis were slightly lower in liver of mice administered with PBA plus CCl_4 as compared with CCl_4 alone (Fig. 2F).

Effects of PBA on CCl_4-induced activation of hepatic NF-κB and MAPK signaling

The effects of PBA on CCl_4-induced hepatic NF-κB activation are shown in Fig. 3A. The level of nuclear NF-κB p65 was significantly increased in liver of mice administered with CCl_4. Interestingly, PBA significantly inhibited CCl_4-induced nuclear translocation of NF-κB p65 (Fig. 3A). The effects of PBA on CCl_4-induced hepatic MAPK signaling were then analyzed. As shown in Figs. 3C and D, the levels of hepatic pERK and pJNK were significantly increased in mice administered with CCl_4. PBA significantly attenuated CCl_4-induced hepatic ERK and JNK phosphorylation. Unexpectedly, the level of hepatic pp38 was significantly decreased in mice administered with CCl_4. PBA had no effect on the level of hepatic pp38 (Fig. 3B). The effects of PBA on CCl_4-induced expression of inflammatory cytokines were analyzed. As expected, long-term CCl_4 administration significantly increased the

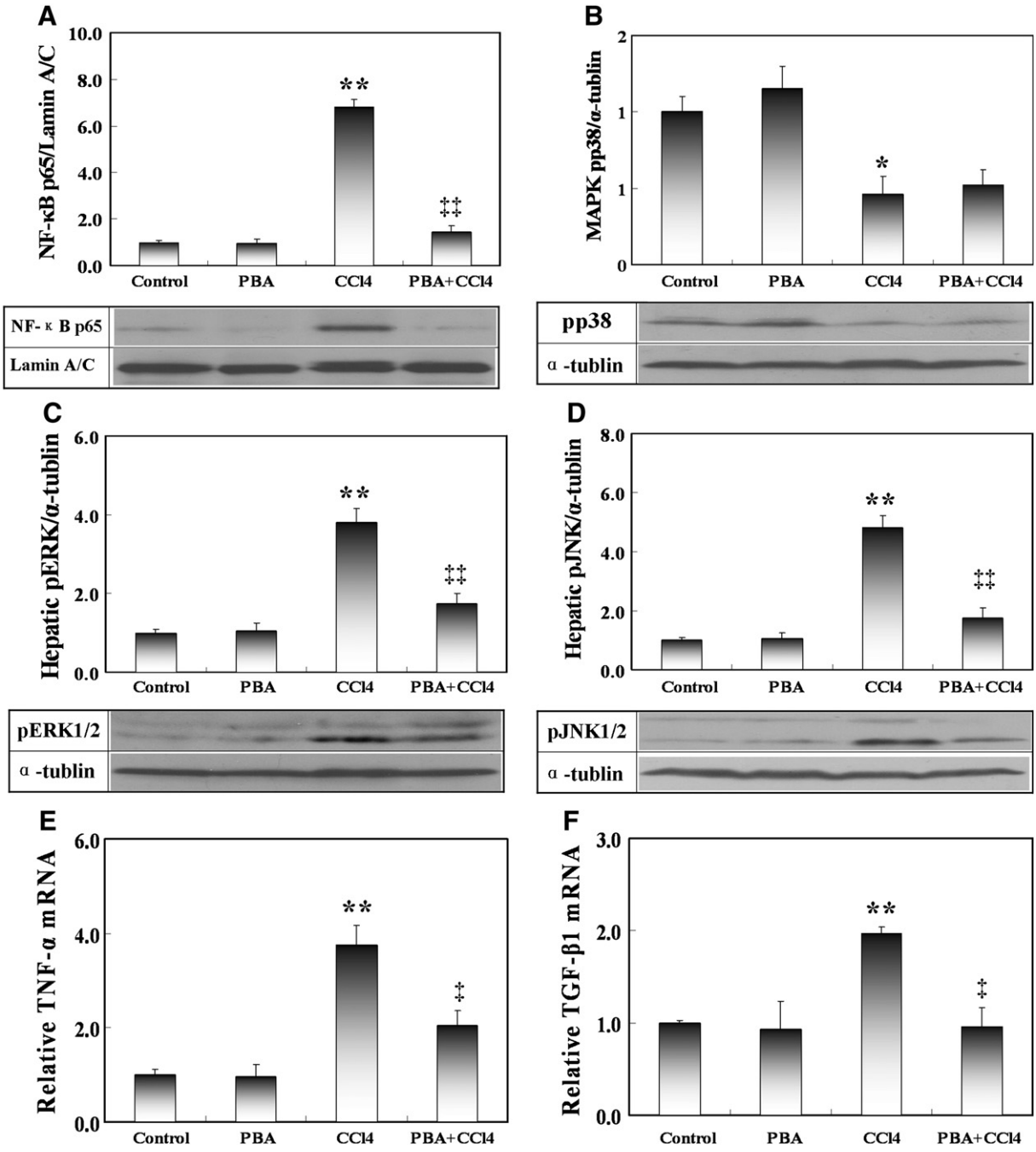

Fig. 3. Effects of PBA on CCl_4-induced activation of NF-κB and MAPK signaling. Mice were intraperitoneally injected with CCl_4 (0.15 ml/kg BW, twice per week) in combination with PBA (150 mg/kg, twice per day) for 8 weeks. Hepatic (A) nuclear NF-κB p65, (B) pp38, (C) pERK and (D) pJNK1/2 were detected using immunobloting. All experiments were repeated for four times. Quantitative analyses of scanning densitometry on four different samples were performed. All proteins were normalized to α-tubulin or lamin A/C level in the same samples. Hepatic (E) *TNF-α* and (F) *TGFβ1* mRNA was detected using real-time RT-PCR. All data were expressed as means ± SE ($n = 6$). $^{*}P<0.05$, $^{**}P<0.01$ as compared with the control. ‡ $P<0.05$, ‡‡ $P<0.01$ as compared with CCl_4 group.

levels of hepatic *TNF-α* and *TGF-β1* mRNAs. Interestingly, PBA significantly attenuated CCl_4-induced upregulation of hepatic *TNF-α* and *TGF-β1* mRNAs (Figs. 3E and F).

PBA attenuates CCl_4-induced expression of hepatic α-SMA

The effects of PBA on CCl_4-induced hepatic α-SMA, a marker associated with HSC activation, were analyzed. Immunohistochemistry showed that α-SMA was mainly distributed in area of liver with bridging fibrosis (Fig. 4B). Further analysis showed that the percentage of α-SMA-positive area was significantly increased in liver of mice administered with CCl_4 (Fig. 4E). PBA significantly attenuated CCl_4-induced hepatic α-SMA (Figs. 4D and F). Correspondingly, the percentage of α-SMA-positive area was significantly decreased in liver of mice administered with PBA plus CCl_4 as compared with CCl_4 alone (Figs. 4D and E).

Effects of PBA on CCl_4-induced expression of hepatic Mmp2, Mmp9, Timp1, Timp2, Col1α1 and Col1α2

The effects of PBA on CCl_4-induced expression of hepatic *Mmp2* and *Mmp9* were analyzed. As shown in Figs. 5A and B, long-term CCl_4 administration significantly upregulated the expression of hepatic *Mmp2* and *Mmp9*. PBA significantly attenuated CCl_4-induced upregulation of hepatic *Mmp2* mRNA (Fig. 5A). The effects of PBA on CCl_4-induced hepatic *Timp1* and *Timp2* are shown in Figs. 5C and D. The levels of hepatic *Timp1* and *Timp2* mRNA were significantly increased in mice administered with CCl_4. PBA significantly attenuated CCl_4-induced upregulation of hepatic *Timp1* mRNA (Fig. 5C). Activated HSCs produce type I collagen molecules. Thus, the effects of PBA on CCl_4-induced hepatic mRNA accumulation of *collagen 1α1* (*Col1a1*) and *Col1a2* were then analyzed. As expected, the levels of

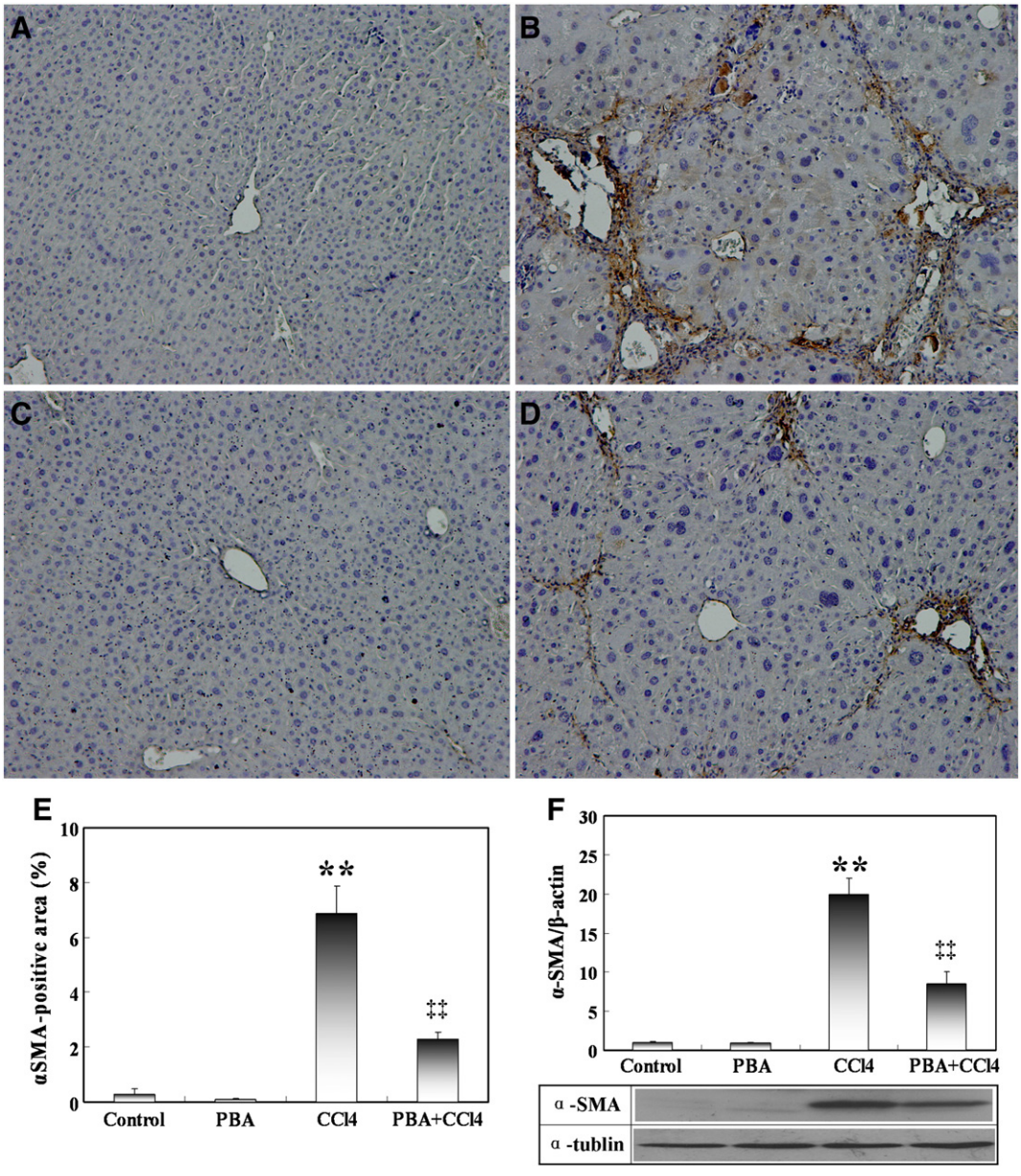

Fig. 4. Effects of PBA on CCl_4-induced expression of hepatic α-SMA. Mice were intraperitoneally injected with CCl_4 (0.15 ml/kg BW, twice per week) in combination with PBA (150 mg/kg, twice per day) for 8 weeks. Representative photomicrographs of liver histology from mice treated with saline (A as control), CCl_4 alone (B), PBA alone (C) and CCl_4 + PBA (D) are shown. Scale bar, 100 μm. (E) Morphometrical analysis was performed for evaluating percentages of a-SMA-positive area in 12 random fields per section. The data were expressed as means ± SE of six animals. (F) Hepatic α-SMA protein was detected by immunoblotting. All experiments were repeated for four times. Quantitative analyses of scanning densitometry on four different samples were performed. α-SMA was normalized to α-tubulin level in the same samples. The data were expressed as means ± SE. $^{**}P<0.01$ as compared with the control. ‡‡ $P<0.01$ as compared with CCl_4 group.

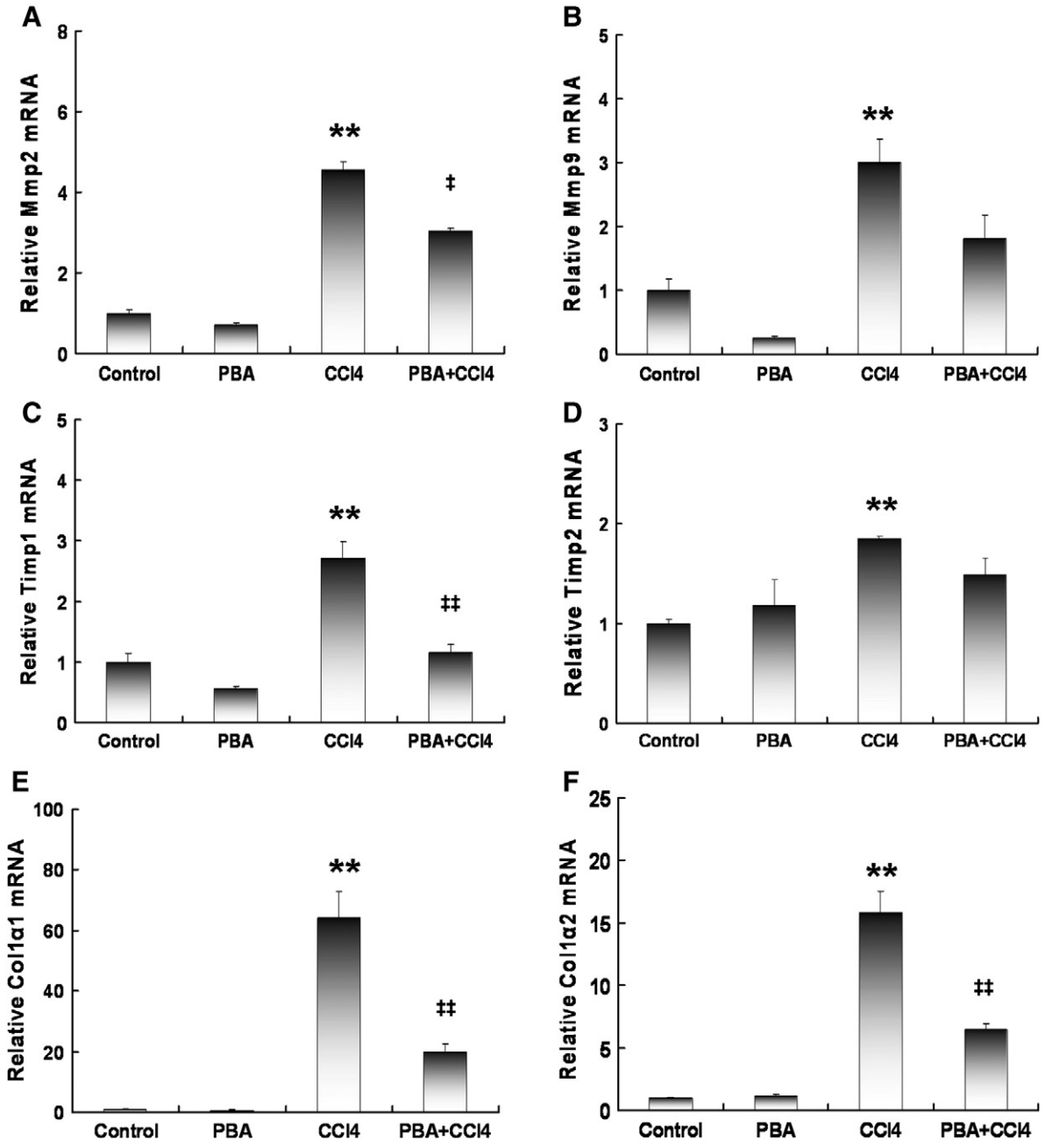

Fig. 5. Effects of PBA on CCl_4-induced expression of hepatic Mmp2, Mmp9, Timp1, Timp2, Col1α1 and Col1α2. Mice were intraperitoneally injected with CCl_4 (0.15 ml/kg BW, twice per week) in combination with PBA (150 mg/kg, twice per day) for 8 weeks. Hepatic (A) *Mmp2*, (B) *Mmp9*, (C) *Timp1*, (D) *Timp2*, (E) *Col1α1* and (F) *Col1α2* mRNA were detected using real-time RT-PCR. The comparative C_T-method was used to determine the amount of target, normalized to an endogenous reference (gapdh) and relative to a calibrator ($2^{-\Delta\Delta Ct}$) using the Lightcycler 480 software (Roche, version 1.5.0). All data were expressed as means ± SE ($n = 6$). $^*P<0.05$, $^{**}P<0.01$ as compared with the control. ‡ $P<0.05$, ‡‡ $P<0.01$ as compared with CCl_4 group.

hepatic *Col1a1* and *Col1a2* mRNAs were obviously increased in mice administered with CCl_4. PBA significantly attenuated CCl_4-induced elevation of hepatic *Col1a1*and *Col1a2* mRNAs (Figs. 5E and F).

PBA alleviates CCl_4-induced hepatic fibrosis

CCl_4-induced hepatic fibrosis was determined using Sirius red staining. As expected, an obvious bridging fibrosis was observed in liver of mice administered with CCl_4 (Fig. 6B). PBA significantly alleviated CCl_4-induced hepatic fibrosis (Fig. 6D). Further analysis showed that the area of hepatic fibrosis was significantly reduced in mice administered with PBA plus CCl_4 as compared with CCl_4 alone (Fig. 6E). The effects of PBA on hepatic hydroxyproline, an indicator of hepatic fibrosis, were then analyzed. Hepatic hydroxyproline content was significantly increased in mice administered with CCl_4. PBA significantly attenuated CCl_4-induced elevation of hepatic hydroxyproline content (Fig. 6F).

Discussion

In the present study, we found that hepatic GRP78, an ER chaperone, was upregulated in CCl_4-treated mice. The level of phosphorylated eIF2α, a downstream molecule of PERK signaling, was significantly increased in the liver of mice injected with CCl_4 for 8 weeks. Hepatic nuclear translocation of ATF6 was observed in mice injected with CCl_4. Hepatic IRE1α signaling was activated by CCl_4. These results

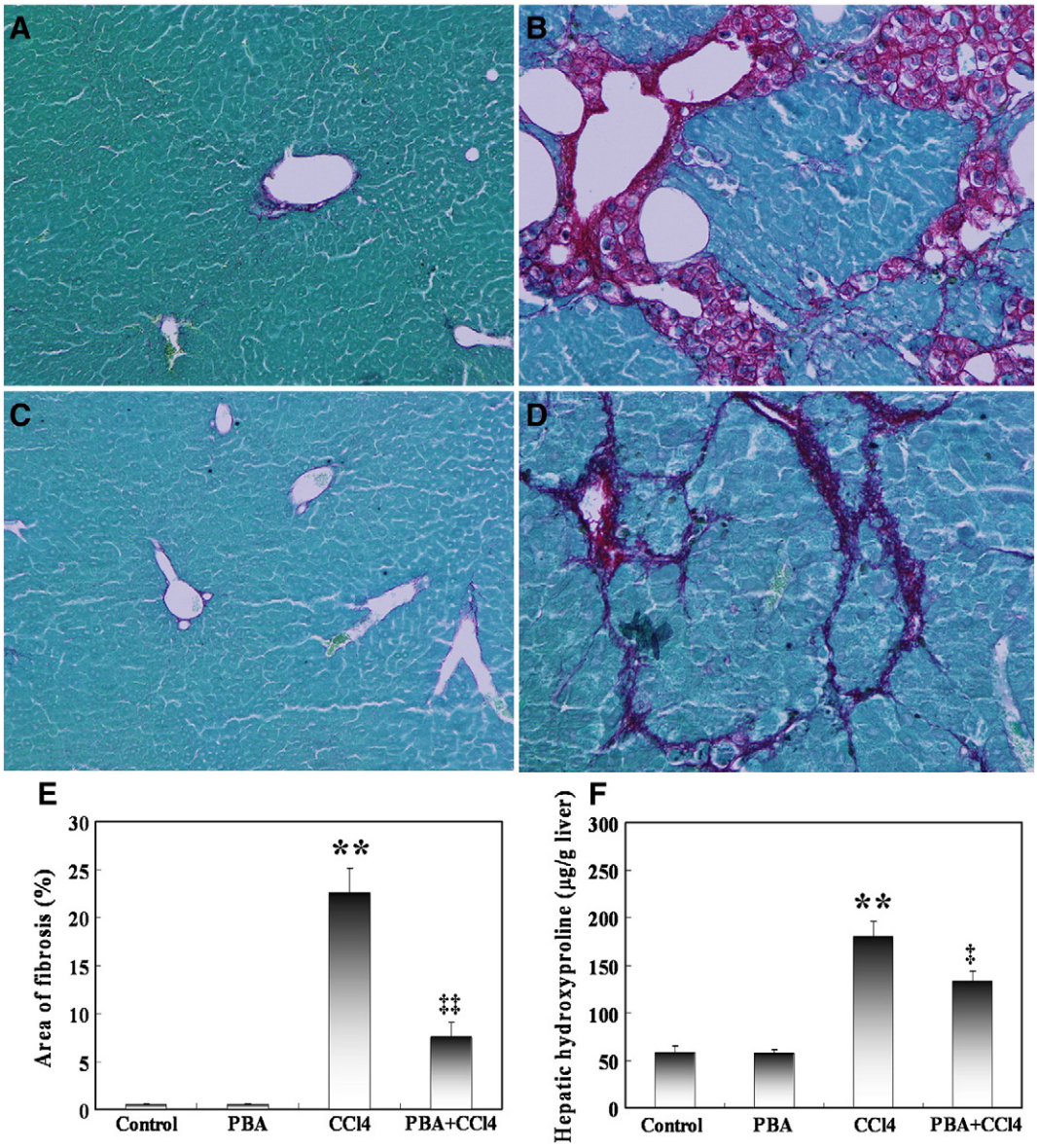

Fig. 6. Effects of PBA on CCl_4-induced hepatic fibrogenesis. Mice were intraperitoneally injected with CCl_4 (0.15 ml/kg BW, twice per week) in combination with PBA (150 mg/kg, twice per day) for 8 weeks. (A–D) Hepatic fibrosis was detected by Sirius Red staining. Representative photomicrographs of liver histology from mice treated with saline (A as control), CCl_4 alone (B), PBA alone (C) and CCl_4 + PBA (D) are shown. Original magnification: 100×. Scale bar, 100 μm. (E) Morphometrical analysis was performed for evaluating percentages of a-SMA-positive area in 12 random fields per section. (F) Hepatic hydroxyproline was detected. All data were expressed as means ± SE of six animals. $^{**}P<0.01$ as compared with the control. ‡ $P<0.05$, ‡‡ $P<0.01$ as compared with CCl_4 group.

are in agreement with those from a recent study (Ji et al., 2011), in which the level of hepatic spliced X-box-binding protein 1 (sXBP-1), a downstream molecule of IRE1α signaling, was increased in mice injected with CCl_4 for 6 weeks. These results suggest that the UPR signaling was activated in the pathogenesis of CCl_4-induced hepatic fibrosis.

Numerous studies demonstrate that PBA, as a chemical chaperone, inhibits ER stress and the UPR signaling (Basseri et al., 2009; Hanada et al., 2007). A recent study showed that PBA significantly downregulated the fibrosis-related genes and protected against cardiac fibrosis in an animal model to produce pressure overload (Park et al., 2012). According to another report, attenuation of ER stress using PBA prevents isoproterenol-induced cardiac fibrosis (Ayala et al., 2012). Recently, a research group investigated the effects of PBA on CCl_4-induced hepatic fibrosis (Ji et al., 2011), in which mice were injected with PBA (1 g/kg, twice per week) for 6 weeks. Unexpectedly, PBA did not protect against CCl_4-induced hepatic fibrosis in wild type mice, whereas this chemical chaperone reduced CCl_4-induced fibrosis by more than 50% in liver-specific GRP78 knockout mice (Ji et al., 2011). In the present study, mice were injected with PBA (150 mg/kg, twice per day) from the beginning of CCl_4 injection to the end. As expected, PBA significantly attenuated CCl_4-induced hepatic ER stress and UPR activation. Surprisingly, this chemical chaperone obviously protected against CCl_4-induced liver fibrosis, whereas it alleviated, only to a less extent, CCl_4-induced hepatic necrosis.

It is widely accepted that the major cellular event in the development and progression of hepatic fibrosis is the activation of HSCs (Fallowfield, 2011; Hernandez-Gea and Friedman, 2011). Indeed, the present study showed that α-SMA, a marker for the initiation phase of HSC activation, was significantly elevated in area of liver with bridging fibrosis. In addition, mRNA levels of hepatic *Col1a1* and

Col1a2, markers for the perpetuation phase of HSC activation, were significantly upregulated in mice administered with CCl_4. These results are in agreement with others (Osterreicher et al., 2009). Recently, several reports showed that ER stress and the UPR signaling activation led to epithelial-to-mesenchymal transition in lung epithelial cells during the pathogenesis of pulmonary fibrosis (Baek et al., 2012; Tanjore et al., 2011; Zhong et al., 2011). In the present study, we showed that CCl_4-induced α-SMA was significantly attenuated in liver of mice pretreated with PBA. In addition, PBA significantly alleviated CCl_4-induced upregulation of hepatic *Col1a1* and *Col1a2* mRNAs. These results suggest that PBA, as an ER chemical chaperone, inhibits HSC activation during the pathogenesis of CCl_4-induced hepatic fibrosis.

Increasing evidence demonstrates that inflammatory cytokines, such as TNF-α and TGF-β, play an important role on HSC activation in the process of hepatic fibrosis (Son et al., 2007). Indeed, the present study showed that the level of hepatic *TNF-α* and *TGF-β1* mRNA was significantly increased in mice injected with CCl_4. Several studies demonstrate that ER stress stimulates the expression of inflammatory mediators through the activation of NF-κB (Hung et al., 2004). Usually, NF-κB is retained in the cytoplasm by binding to I-κB. Under ER stress, NF-κB is translocated to the nucleus through translational inhibition of Iκ-B synthesis (Wu et al., 2004). An earlier report demonstrates that eIF2α phosphorylation is required for NF-κB activation in response to ER stress (Jiang et al., 2003). Indeed, the present study showed that CCl_4-induced eIF2α phosphorylation was significantly alleviated in liver of mice pretreated with PBA. Correspondingly, CCl_4-induced hepatic NF-κB p65 translocation was inhibited in mice pretreated with PBA. Moreover, CCl_4-induced hepatic TNF-α and TGF-β1 unregulation was attenuated by PBA. These results suggest that PBA represses CCl_4-induced HSC activation through inhibiting NF-κB activation and subsequent inflammatory response.

JNK, a member of the mitogen-activated protein kinase (MAPK) family, is involved in the regulation of inflammation (Gunawan et al., 2006; Henderson et al., 2007). Indeed, JNK mediates HSC activation in the pathogenesis of liver fibrosis (Kluwe et al., 2010). According to several reports from different laboratories, IRE1, a transmembrane ER protein that contains a cytoplasmic kinase, links ER stress to JNK phosphorylation (Nishitoh et al., 2002; Urano et al., 2000). A recent study found that activating transcription factor 4 (ATF4), another downstream target of PERK signaling, upregulated inflammatory cytokines through the activation of JNK (Zhong et al., 2012). The present study showed that pretreatment with PBA significantly attenuated CCl_4-induced hepatic JNK phosphorylation. Thus, it is proposed that PBA represses CCl_4-induced hepatic inflammatory response and HSC activation through inhibiting hepatic MAPK signaling.

In the present study, we laid emphasis on the effects of PBA on hepatic inflammatory response and HSC activation in the pathogenesis of CCl_4-induced hepatic fibrosis. The present study has several limitations. First, the present study only investigated the effects of a single dose PBA on CCl_4-induced HSC activation and hepatic fibrosis. Second, the present study only investigated the effects of pretreatment with PBA on CCl_4-induced hepatic fibrosis. Thus, additional work is required to determine a dose response curve to assess the effects of different doses PBA on CCl_4-induced HSC activation and hepatic fibrosis. In addition, the anti-fibrotic effects of PBA need to be demonstrated in different models of liver fibrosis.

In summary, the present study demonstrates that the UPR signaling is activated in the pathogenesis of CCl_4-induced hepatic fibrosis. PBA, a well-known ER chemical chaperone, inhibits CCl_4-induced hepatic ER stress and the UPR signaling. Moreover, PBA alleviates CCl_4-induced hepatic NF-κB translocation and MAPK signaling. In addition, PBA attenuates CCl_4-induced inflammatory response and subsequent HSC activation. Importantly, PBA effectively prevents CCl_4-induced hepatic fibrosis in mice (Fig. 7). Thus, chemical chaperone may have potential preventive and therapeutic utilities for protecting against liver fibrosis.

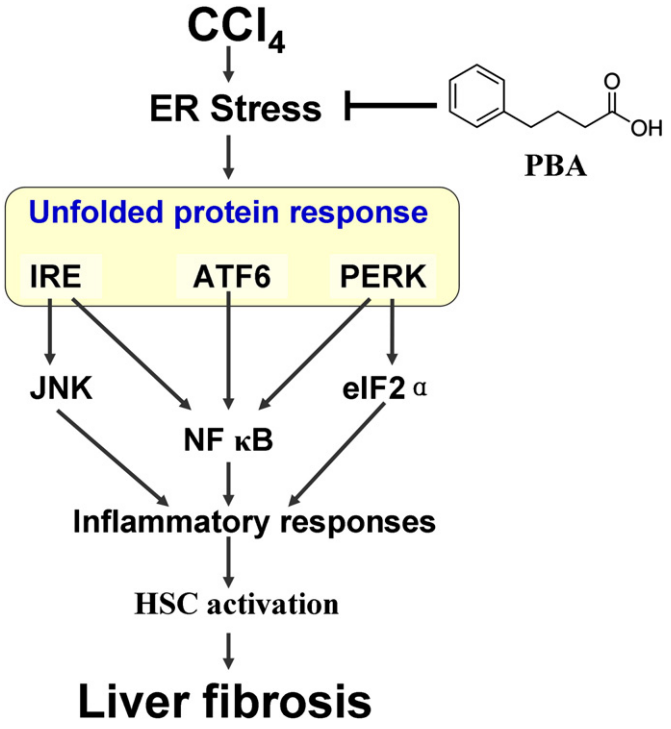

Fig. 7. Phenylbutyric acid protects against carbon tetrachloride-induced hepatic fibrogenesis. Long-term CCl_4 administration induces hepatic ER stress and UPR signaling activation, which may play an important role on CCl_4-induced inflammation, HSC activation and subsequent hepatic fibrosis. PBA, an ER chemical chaperone, inhibits CCl_4-induced hepatic ER stress and UPR signaling. Moreover, PBA alleviates CCl_4-induced inflammation through its inhibition of NF-κB activation and JNK phosphorylation. Finally, PBA effectively protects against CCl_4-induced HSC activation and hepatic fibrosis.

Conflict of interest statement

The authors declare that there are no conflicts of interest.

Acknowledgments

This project was supported by National Natural Science Foundation of China (30371667, 30572223, 30973544, 81172711, 81001480), Natural Science Foundation of Anhui province (090413142, 1208085QH143) and the University Excellence Young Talent Fund of Educational Commission of Anhui Province (2011SQRL058).

References

Ayala, P., Montenegro, J., Vivar, R., Letelier, A., Urroz, P.A., Copaja, M., Pivet, D., Humeres, C., Troncoso, R., Vicencio, J.M., Lavandero, S., Díaz-Araya, G., 2012. Attenuation of endoplasmic reticulum stress using the chemical chaperone 4-phenylbutyric acid prevents cardiac fibrosis induced by isoproterenol. Exp. Mol. Pathol. 92, 97–104.

Baek, H.A., Kim do, S., Park, H.S., Jang, K.Y., Kang, M.J., Lee, D.G., Moon, W.S., Chae, H.J., Chung, M.J., 2012. Involvement of endoplasmic reticulum stress in myofibroblastic differentiation of lung fibroblasts. Am. J. Respir. Cell Mol. Biol. 46, 731–739.

Basseri, S., Lhotak, S., Sharma, A.M., Austin, R.C., 2009. The chemical chaperone 4-phenylbutyrate inhibits adipogenesis by modulating the unfolded protein response. J. Lipid Res. 50, 2486–2501.

Bataller, R., Brenner, D.A., 2005. Liver fibrosis. J. Clin. Invest. 115, 209–218.

Ben Mosbah, I., Alfany-Fernandez, I., Martel, C., Zaouali, M.A., Bintanel-Morcillo, M., Rimola, A., Rodes, J., Brenner, C., Rosello-Catafau, J., Peralta, C., 2010. Endoplasmic reticulum stress inhibition protects steatotic and non-steatotic livers in partial hepatectomy under ischemia–reperfusion. Cell Death Dis. 1, e52.

Burlina, A.B., Ogier, H., Korall, H., Trefz, F.K., 2001. Long-term treatment with sodium phenylbutyrate in ornithine transcarbamylase-deficient patients. Mol. Genet. Metab. 72, 351–355.

Dara, L., Ji, C., Kaplowitz, N., 2011. The contribution of endoplasmic reticulum stress to liver diseases. Hepatology 53, 1752–1763.

Fallowfield, J.A., 2011. Therapeutic targets in liver fibrosis. Am. J. Physiol. Gastrointest. Liver Physiol. 300, G709–G715.

Fracanzani, A.L., Valenti, L., Bugianesi, E., Vanni, E., Grieco, A., Miele, L., Consonni, D., Fatta, E., Lombardi, R., Marchesini, G., Fargion, S., 2011. Risk of nonalcoholic steatohepatitis and fibrosis in patients with nonalcoholic fatty liver disease and low visceral adiposity. J. Hepatol. 54, 1244–1249.

Friedman, S.L., 2010. Evolving challenges in hepatic fibrosis. Nat. Rev. Gastroenterol. Hepatol. 7, 425–436.

Gunawan, B.K., Liu, Z.X., Han, D., Hanawa, N., Gaarde, W.A., Kaplowitz, N., 2006. c-Jun N-terminal kinase plays a major role in murine acetaminophen hepatotoxicity. Gastroenterology 131, 165–178.

Hanada, S., Harada, M., Kumemura, H., Bishr Omary, M., Koga, H., Kawaguchi, T., Taniguchi, E., Yoshida, T., Hisamoto, T., Yanagimoto, C., Maeyama, M., Ueno, T., Sata, M., 2007. Oxidative stress induces the endoplasmic reticulum stress and facilitates inclusion formation in cultured cells. J. Hepatol. 47, 93–102.

Henderson, N.C., Pollock, K.J., Frew, J., Mackinnon, A.C., Flavell, R.A., Davis, R.J., Sethi, T., Simpson, K.J., 2007. Critical role of c-jun (NH2) terminal kinase in paracetamol-induced acute liver failure. Gut 56, 982–990.

Hernandez-Gea, V., Friedman, S.L., 2011. Pathogenesis of liver fibrosis. Annu. Rev. Pathol. 6, 425–456.

Hung, J.H., Su, I.J., Lei, H.Y., Wang, H.C., Lin, W.C., Chang, W.T., Huang, W., Chang, W.C., Chang, Y.S., Chen, C.C., Lai, M.D., 2004. Endoplasmic reticulum stress stimulates the expression of cyclooxygenase-2 through activation of NF-kappaB and pp 38 mitogen-activated protein kinase. J. Biol. Chem. 279, 46384–46392.

Ji, C., Kaplowitz, N., Lau, M.Y., Kao, E., Petrovic, L.M., Lee, A.S., 2011. Liver-specific loss of glucose-regulated protein 78 perturbs the unfolded protein response and exacerbates a spectrum of liver diseases in mice. Hepatology 54, 229–239.

Jiang, H.Y., Wek, S.A., McGrath, B.C., Scheuner, D., Kaufman, R.J., Cavener, D.R., Wek, R.C., 2003. Phosphorylation of the alpha subunit of eukaryotic initiation factor 2 is required for activation of NF-kappaB in response to diverse cellular stresses. Mol. Cell. Biol. 23, 5651–5663.

Kluwe, J., Pradere, J.P., Gwak, G.Y., Mencin, A., De Minicis, S., Osterreicher, C.H., Colmenero, J., Bataller, R., Schwabe, R.F., 2010. Modulation of hepatic fibrosis by c-Jun-N-terminal kinase inhibition. Gastroenterology 138, 347–359.

Kohno, K., 2007. How transmembrane proteins sense endoplasmic reticulum stress. Antioxid. Redox Signal. 9, 2295–2303.

Lee, G.H., Bhandary, B., Lee, E.M., Park, J.K., Jeong, K.S., Kim, I.K., Kim, H.R., Chae, H.J., 2011. The roles of ER stress and P450 2E1 in CCl(4)-induced steatosis. Int. J. Biochem. Cell Biol. 43, 1469–1482.

Mallat, A., Hezode, C., Lotersztajn, S., 2008. Environmental factors as disease accelerators during chronic hepatitis C. J. Hepatol. 48, 657–665.

Mencin, A., Seki, E., Osawa, Y., Kodama, Y., De Minicis, S., Knowles, M., Brenner, D.A., 2007. Alpha-1 antitrypsin Z protein (PiZ) increases hepatic fibrosis in a murine model of cholestasis. Hepatology 46, 1443–1452.

Moustafa, T., Fickert, P., Magnes, C., Guelly, C., Thueringer, A., Frank, S., Kratky, D., Sattler, W., Reicher, H., Sinner, F., Gumhold, J., Silbert, D., Fauler, G., Hofler, G., Lass, A., Zechner, R., Trauner, M., 2012. Alterations in lipid metabolism mediate inflammation, fibrosis, and proliferation in a mouse model of chronic cholestatic liver injury. Gastroenterology 142 (140–151), e112.

Nishitoh, H., Matsuzawa, A., Tobiume, K., Saegusa, K., Takeda, K., Inoue, K., Hori, S., Kakizuka, A., Ichijo, H., 2002. ASK1 is essential for endoplasmic reticulum stress-induced neuronal cell death triggered by expanded polyglutamine repeats. Genes Dev. 16, 1345–1355.

Odievre, M.H., Brun, M., Krishnamoorthy, R., Lapoumeroulie, C., Elion, J., 2007. Sodium phenyl butyrate downregulates endothelin-1 expression in cultured human endothelial cells: relevance to sickle-cell disease. Am. J. Hematol. 82, 357–362.

Osterreicher, C.H., Taura, K., De Minicis, S., Seki, E., Penz-Osterreicher, M., Kodama, Y., Kluwe, J., Schuster, M., Oudit, G.Y., Penninger, J.M., Brenner, D.A., 2009. Angiotensin-converting-enzyme 2 inhibits liver fibrosis in mice. Hepatology 50, 929–938.

Ozcan, U., Yilmaz, E., Ozcan, L., Furuhashi, M., Vaillancourt, E., Smith, R.O., Gorgun, C.Z., Hotamisligil, G.S., 2006. Chemical chaperones reduce ER stress and restore glucose homeostasis in a mouse model of type 2 diabetes. Science 313, 1137–1140.

Ozcan, L., Ergin, A.S., Lu, A., Chung, J., Sarkar, S., Nie, D., Myers Jr., M.G., Ozcan, U., 2009. Endoplasmic reticulum stress plays a central role in development of leptin resistance. Cell Metab. 9, 35–51.

Park, C.S., Cha, H., Kwon, E.J., Sreenivasaiah, P.K., Kim do, H., 2012. The chemical chaperone 4-phenylbutyric acid attenuates pressure-overload cardiac hypertrophy by alleviating endoplasmic reticulum stress. Biochem. Biophys. Res. Commun. 421, 578–584.

Reddy, G.K., Enwemeka, C.S., 1996. A simplified method for the analysis of hydroxyproline in biological tissues. Clin. Biochem. 29, 225–229.

Son, G., Iimuro, Y., Seki, E., Hirano, T., Kaneda, Y., Fujimoto, J., 2007. Selective inactivation of NF-kappaB in the liver using NF-kappaB decoy suppresses CCl4-induced liver injury and fibrosis. Am. J. Physiol. Gastrointest. Liver Physiol. 293, G631–G639.

Tamaki, N., Hatano, E., Taura, K., Tada, M., Kodama, Y., Nitta, T., Iwaisako, K., Seo, S., Nakajima, A., Ikai, I., Uemoto, S., 2008. CHOP deficiency attenuates cholestasis-induced liver fibrosis by reduction of hepatocyte injury. Am. J. Physiol. Gastrointest. Liver Physiol. 294, G498–G505.

Tanjore, H., Cheng, D.S., Degryse, A.L., Zoz, D.F., Abdolrasulnia, R., Lawson, W.E., Blackwell, T.S., 2011. Alveolar epithelial cells undergo epithelial-to-mesenchymal transition in response to endoplasmic reticulum stress. J. Biol. Chem. 286, 30972–30980.

Urano, F., Wang, X., Bertolotti, A., Zhang, Y., Chung, P., Harding, H.P., Ron, D., 2000. Coupling of stress in the ER to activation of JNK protein kinases by transmembrane protein kinase IRE1. Science 287, 664–666.

Wu, J., Kaufman, R.J., 2006. From acute ER stress to physiological roles of the Unfolded Protein Response. Cell Death Differ. 13, 374–384.

Wu, S., Tan, M., Hu, Y., Wang, J.L., Scheuner, D., Kaufman, R.J., 2004. Ultraviolet light activates NFkappaB through translational inhibition of IkappaBalpha synthesis. J. Biol. Chem. 279, 34898–34902.

Xiao, C., Giacca, A., Lewis, G.F., 2011. Sodium phenylbutyrate, a drug with known capacity to reduce endoplasmic reticulum stress, partially alleviates lipid-induced insulin resistance and beta-cell dysfunction in humans. Diabetes 60, 918–924.

Zhong, Q., Zhou, B., Ann, D.K., Minoo, P., Liu, Y., Banfalvi, A., Krishnaveni, M.S., Dubourd, M., Demaio, L., Willis, B.C., Kim, K.J., duBois, R.M., Crandall, E.D., Beers, M.F., Borok, Z., 2011. Role of endoplasmic reticulum stress in epithelial–mesenchymal transition of alveolar epithelial cells: effects of misfolded surfactant protein. Am. J. Respir. Cell Mol. Biol. 45, 498–509.

Zhong, Y., Li, J., Chen, Y., Wang, J.J., Ratan, R., Zhang, S.X., 2012. Activation of endoplasmic reticulum stress by hyperglycemia is essential for Muller cell-derived inflammatory cytokine production in diabetes. Diabetes 61, 492–504.